

SUPPORTING INFORMATION

Face-on Reorientation of π -Conjugated Polymers in Thin Films by Surface-Segregated Monolayers

Wei-Chih Wang^{a,b,d}, Sheng-Yuan Chen^{c,e}, Yaw-Wen Yang^{c,e,}, Chain-Shu Hsu^{b,d,*},
Keisuke Tajima^{a,*}*

^aRIKEN Center for Emergent Matter Science (CEMS), 2-1 Hirosawa, Wako, Saitama 351-0198, Japan.

^bDepartment of Applied Chemistry, National Chiao Tung University, 1001 University Rd., Hsinchu 30010, Taiwan

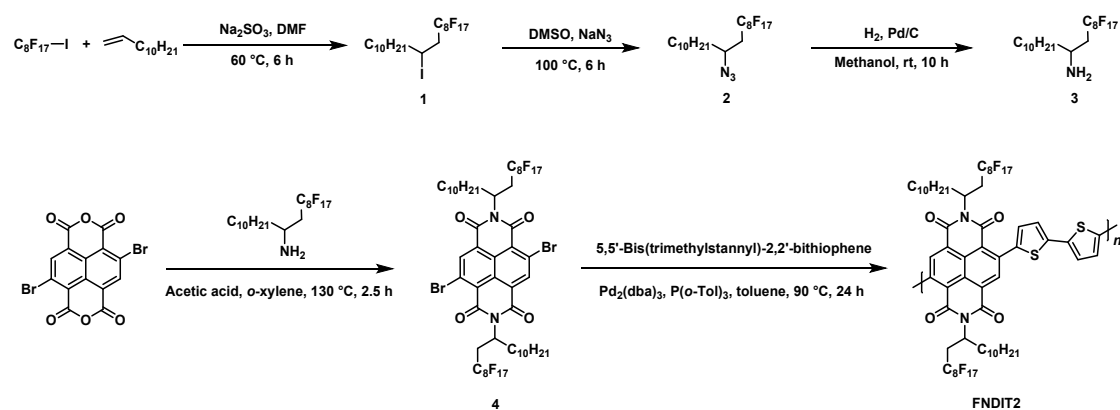
^cNational Synchrotron Radiation Research Center, Hsinchu 30076, Taiwan.

^dCenter for Emergent Functional Matter Science, National Chiao Tung University, 1001 University Rd., Hsinchu 30010, Taiwan.

^eDepartment of Chemistry, National Tsing-Hua University, Hsinchu 30013, Taiwan

Synthesis

All the chemicals and solvent are commercially available and used without purification unless otherwise noted.



Scheme 1. Synthetic route for FNDIT2.

1,1,1,2,2,3,3,4,4,5,5,6,6,7,7,8,8-Heptafluoro-10-iodoicosane (1). 1-Dodecene (15.41 g, 91.58 mmol), 1,1,1,2,2,3,3,4,4,5,5,6,6,7,7,8,8-heptafluoro-8-iodooctane (25 g, 45.79 mmol), and Na_2SO_3 (9.23 g, 73.26 mmol) were dissolved in DMF (160 mL). The mixture was heated at $60\text{ }^\circ\text{C}$ for 6 h under N_2 . The solution was extracted with CH_2Cl_2 and washed with water, and the organic layer was dried with $MgSO_4$ and concentrated by evaporation. The liquid product was purified by column chromatography using hexane as the eluent. Distillation of the mixture afforded the product as a clear liquid (26.3 g, 80%). 1H NMR (400 MHz, $CDCl_3$): δ 4.33 (m, 1H), 2.83

(m, 2H), 1.79 (m, 2H), 1.30 (br, 16H), 0.88 (t, $J = 6.8$ Hz, 3H).

10-Azido-1,1,1,2,2,3,3,4,4,5,5,6,6,7,7,8,8-heptadecafluoricosane (2). NaN₃ (1.36 g, 20.99 mmol) was added in one portion to a solution of **1** (3 g, 4.19 mmol) in DMSO (15 mL). The mixture was heated at 60 °C for 1 day. The solution was extracted with CH₂Cl₂ and washed with water. The organic layer was dried with MgSO₄ and concentrated by evaporation. The product was purified by column chromatography using hexane as the eluent, and the product was obtained as a clear liquid (960 mg, 36%). ¹H NMR (400 MHz, CDCl₃): δ 3.74 (m, 1H), 2.24 (m, 2H), 1.61 (m, 2H), 1.35 (br, 16H), 0.88 (t, $J = 6.8$ Hz, 3H). HRMS (FI⁺) calculated for C₂₀H₂₄F₁₇N₃ [M⁺], 629.16988; found, 629.16622.

13,13,14,14,15,15,16,16,17,17,18,18,19,19,20,20,20-Heptadecafluoricosan-11-amine (3). **2** (1.5 g, 2.38 mmol) and Pd/C (60 mg) were dispersed in MeOH (7.5 mL), and the mixture was stirred overnight under H₂. The crude product was purified by column chromatography using CH₂Cl₂/hexane (2:1) as the eluent to afford the product as a white solid (1.25 g, 87%). ¹H NMR (400 MHz, CDCl₃): δ 3.30 (m, 1H), 2.10 (m, 2H), 1.40 (br, 20H), 0.88 (t, $J = 6.8$ Hz, 3H). HRMS (FI⁺) calculated for C₂₀H₂₆F₁₇N [M⁺], 603.17938; found, 603.17945.

Compound 4. 3 (2.12 g, 3.52 mmol) and 2,6-dibromonaphthalene-1,4,5,8-tetracarboxylic dianhydride (500 mg, 1.17 mmol) were dissolved in *o*-xylene (20 mL). Acetic acid (7.5 mL) was added slowly to the solution, and the mixture was stirred at 130 °C for 2.5 h. The solution was extracted with CH₂Cl₂ and washed with water. The organic layer was dried with MgSO₄ and concentrated by evaporation. The crude product was separated by column chromatography using CH₂Cl₂/hexane (1:2) as the eluent to afford the product as a light yellow solid (400 mg, 21%). ¹H NMR (400 MHz, CDCl₃): δ 9.03 (d, *J* = 26.8 Hz, 2H), 5.66 (m, 2H), 3.28 (m, 2H), 2.58 (m, 2H), 2.27 (br, 2H), 1.89 (br, 2H), 1.24 (br, 32H), 0.85 (t, *J* = 6.8 Hz, 3H); HRMS (FD) calculated for C₅₄H₅₀Br₂F₃₄N₂O₄ [M⁺], 1596.15739; found, 1596.15179.

FNDIT2. 4 (150 mg, 0.094 mmol), 5,5'-bis(trimethylstannyl)-2,2'-bithiophene (46.2 mg, 0.094 mmol), Pd₂(dba)₃ (3.44 mg), and tri(*o*-tolyl)phosphine (4.57 mg) were dissolved in anhydrous toluene (3.76 mL) and the solution was stirred under N₂ at 90 °C for 24 h. After cooling to room temperature, the solution was poured into MeOH. The blue solid was purified further by Soxhlet extraction with MeOH, acetone, and hexane sequentially for 12 h each. The remaining solid was dissolved in CHCl₃ and reprecipitated into MeOH. The precipitate was collected by filtration and dried under vacuum. The product was obtained as blue solid (120 mg, 80%) (*M*_n = 20,000, *M*_w =

29,000, PDI = 1.43).

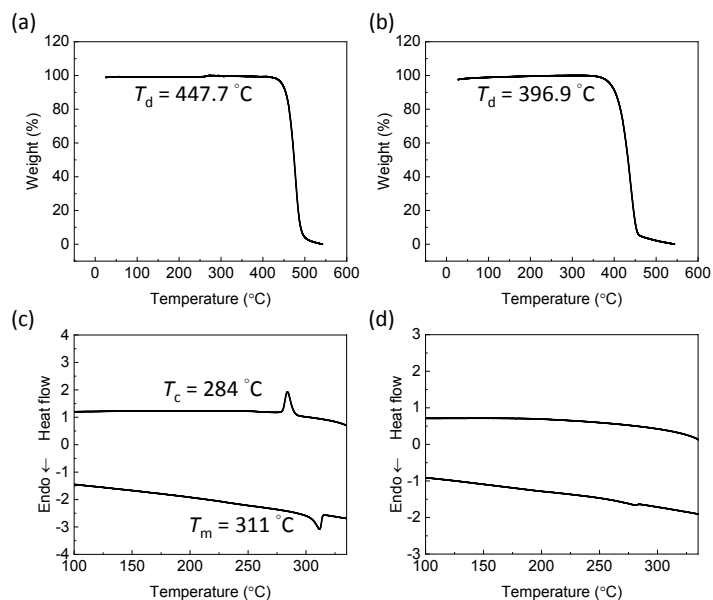


Fig. S1 Thermogravimetric analysis of (a) N2200 and (b) FNDIT2 and DSC traces of (c) N2200 and (d) FNDIT2. The heating and the cooling rates were 10 K min^{-1} . T_d : decomposition temperature; T_c : crystallization temperature; T_m : melting temperature.

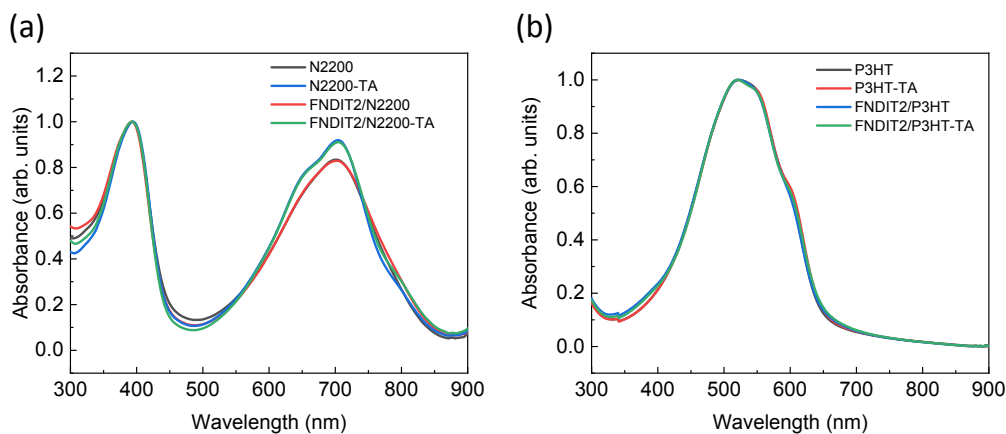


Fig. S2 (a) Normalized UV-Vis spectra of N2200 and FNDIT2/N2200 films (TA indicates after annealing at $260 \text{ }^\circ\text{C}$ for 30 min). (b) Normalized UV-Vis spectra of P3HT and FNDIT2/P3HT films (TA indicates after annealing at $100 \text{ }^\circ\text{C}$ for 10 min).

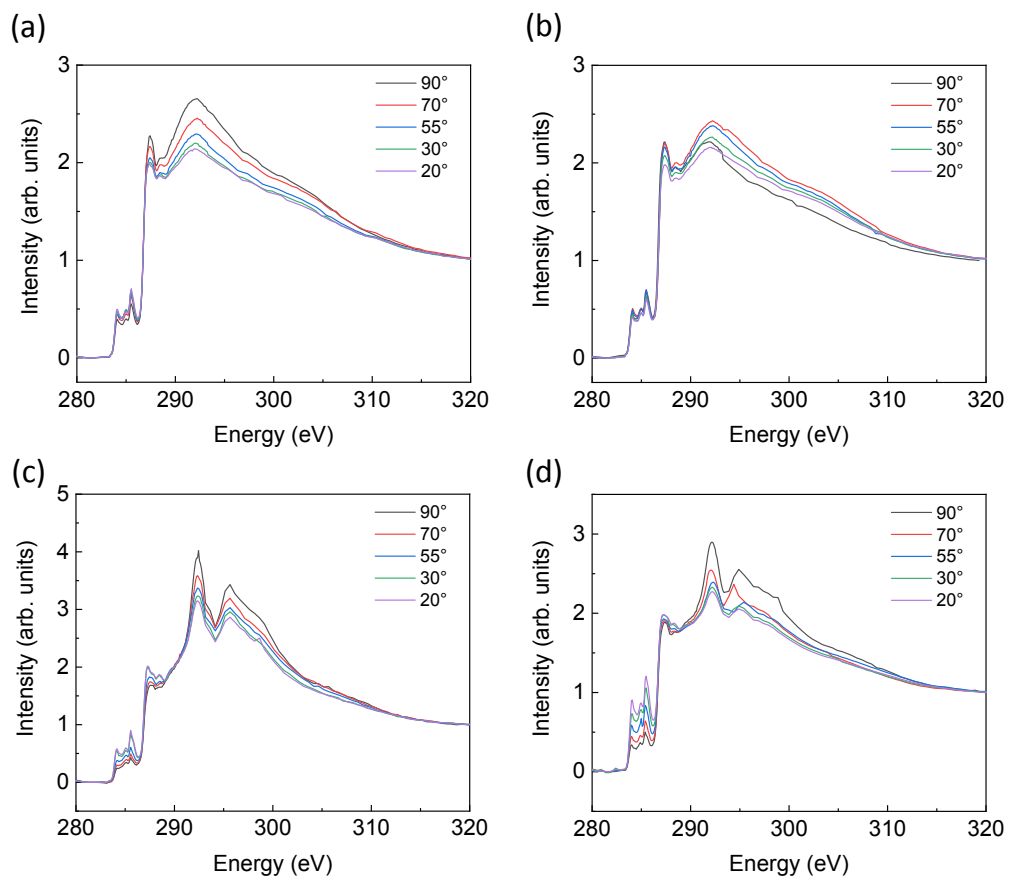


Fig. S3 Angle-resolved NEXAFS spectra of (a) N2200, (b) N2200 (after thermal annealing), (c) FNDIT2/N2200, and (d) FNDIT2/N2200 films (after thermal annealing).

The data were collected in AEY mode.

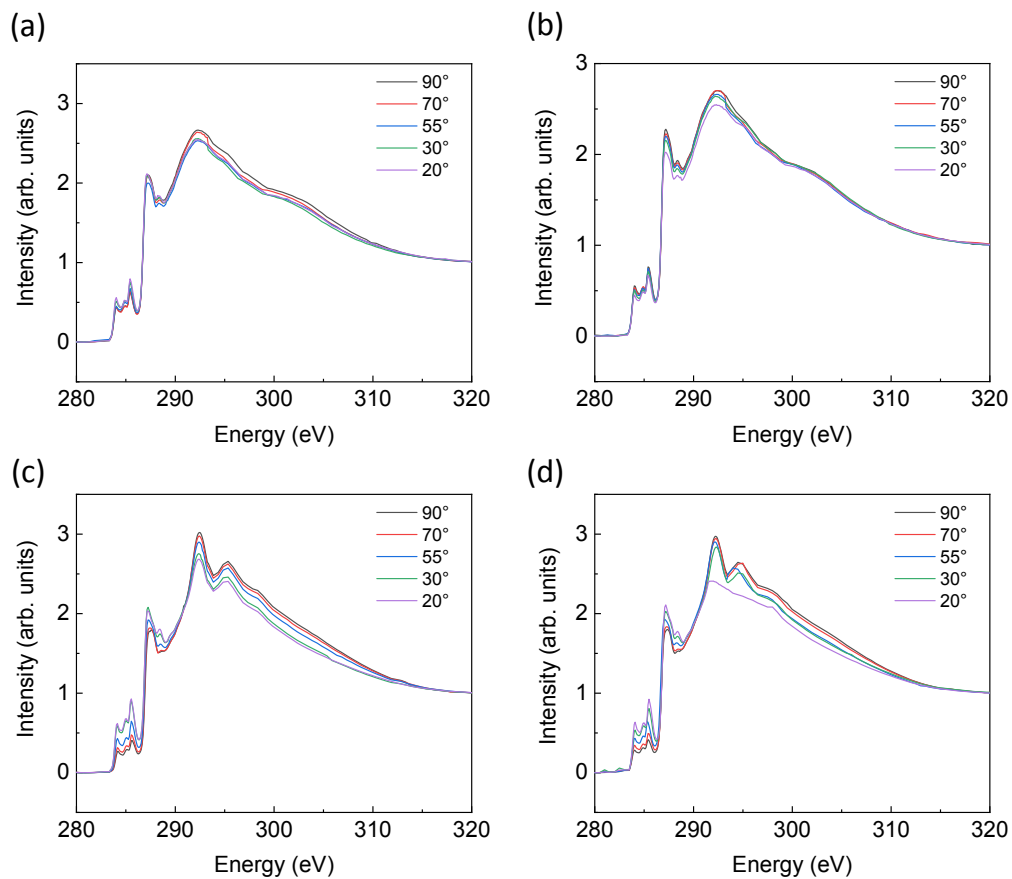


Fig. S4 Angle-resolved NEXAFS spectra of (a) N2200, (b) N2200 (after thermal annealing), (c) FNDIT2/N2200, and (d) FNDIT2/N2200 films (after thermal annealing).

The data were collected in TEY mode.

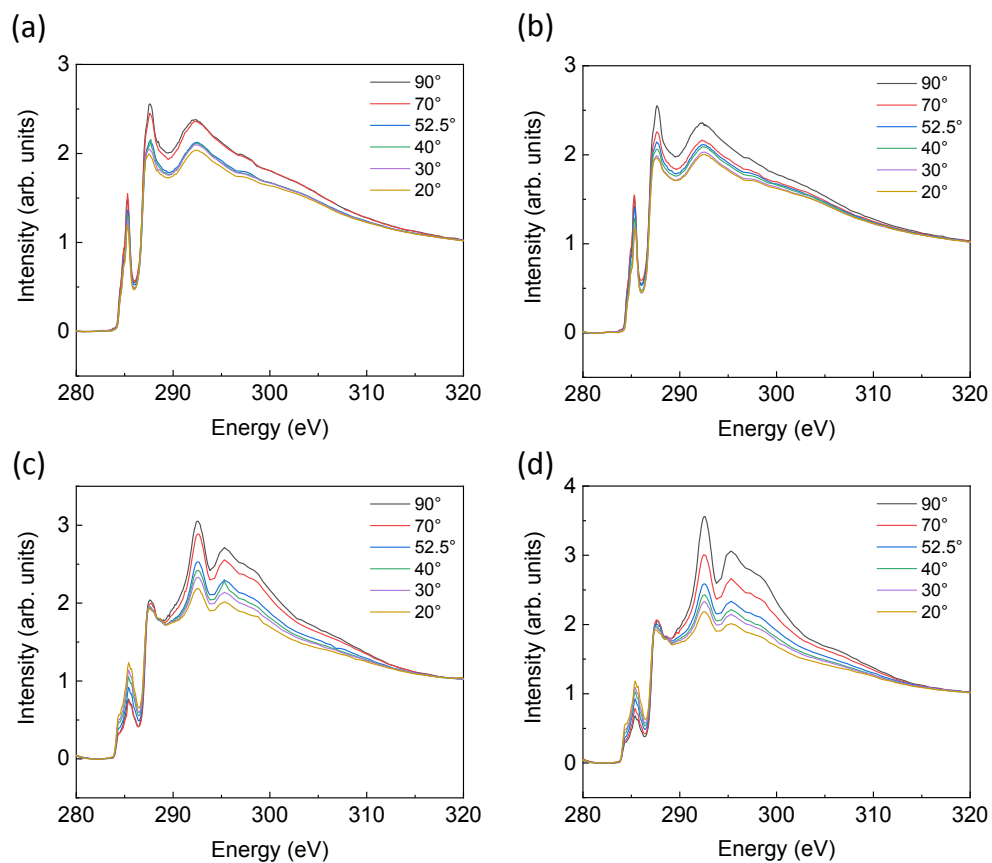


Fig. S5 Angle-resolved NEXAFS spectra of (a) P3HT, (b) P3HT (after thermal annealing), (c) FNDIT2/P3HT, and (d) FNDIT2/P3HT films (after thermal annealing). The data were collected in AEY mode.

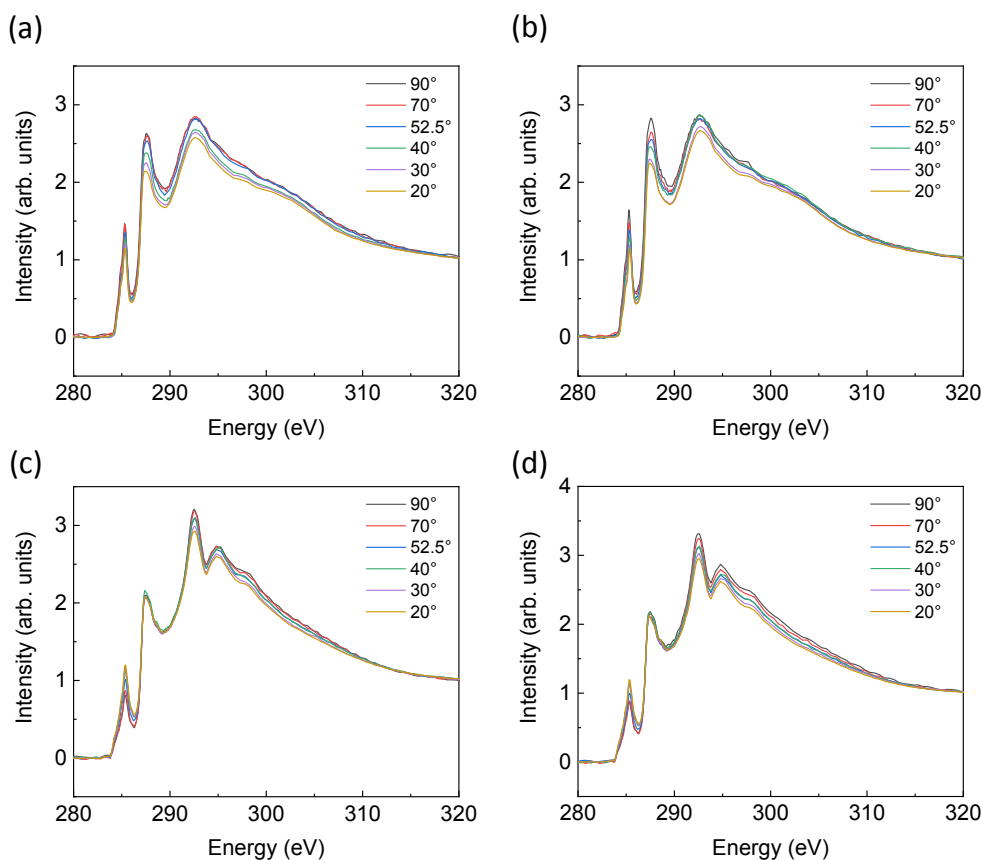


Fig. S6 Angle-resolved NEXAFS spectra of (a) P3HT, (b) P3HT (after thermal annealing), (c) FNDIT2/P3HT, and (d) FNDIT2/P3HT films (after thermal annealing). The data were collected in TEY mode.

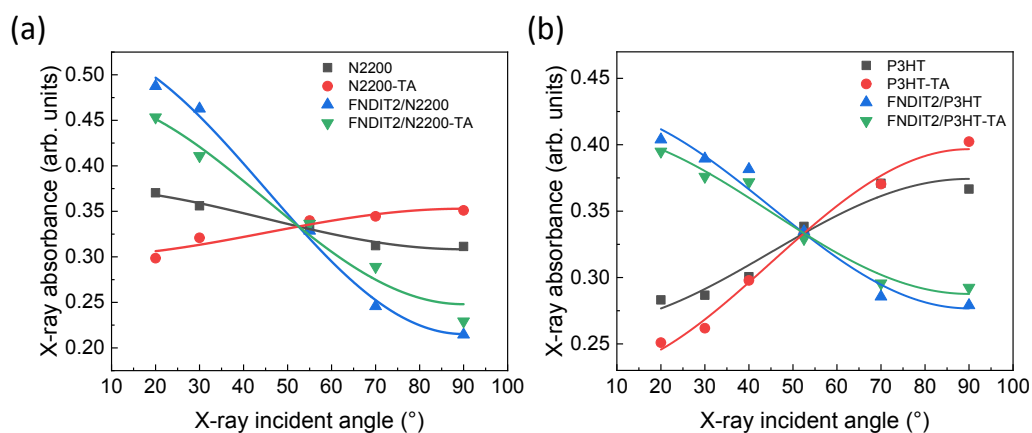


Fig. S7 Integrated intensity of the C 1s to π^* transitions in the range of 283–286.5 eV plotted against the X-ray incident angle (ϑ) for (a) N2200 and FNDIT2/N2200 films and

(b) P3HT and FNDIT2/P3HT films before and after thermal annealing (TA indicates after annealing at 260 °C for 30 min for FNDIT2/N2200 and at 100 °C for 10 min for FNDIT2/P3HT). The detections are in TEY mode. The curves are best fits of the data to Eq. 1.

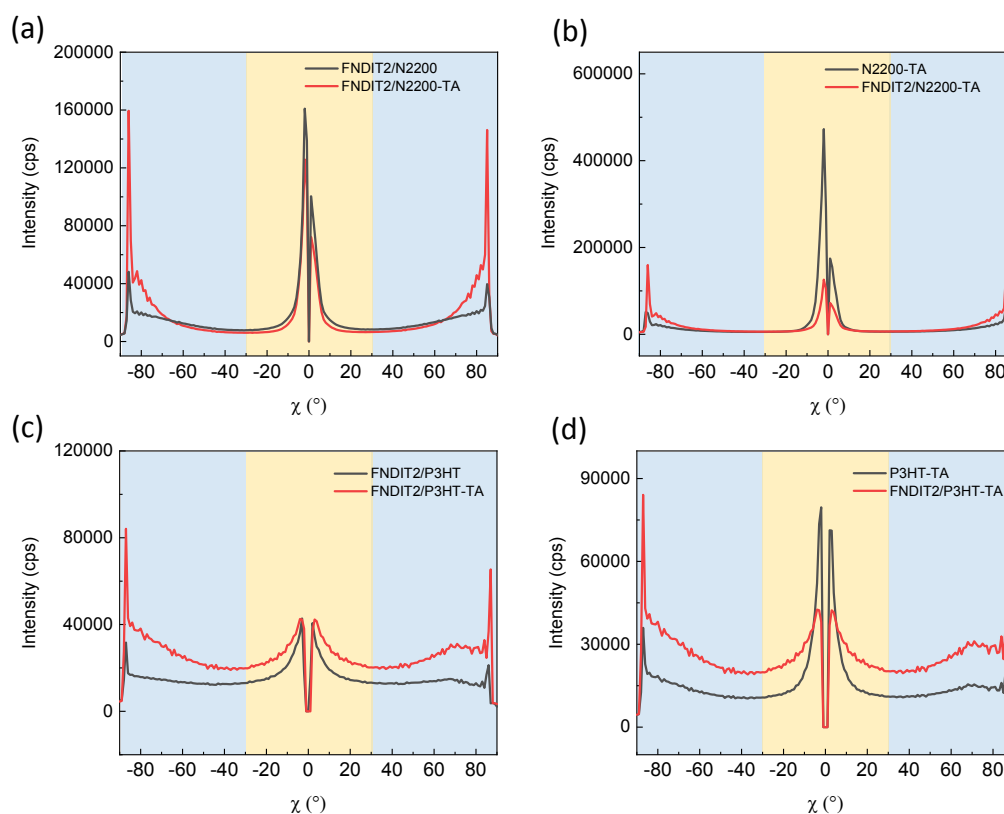


Fig. S8 Pole Fig plots obtained from the GIWAXS diffraction patterns for (a) FNDIT2/N2200 before and after thermal annealing, (b) N2200 and FNDIT2/N2200 after thermal annealing, (c) FNDIT2/P3HT before and after thermal annealing, (d) P3HT and FNDIT2/ P3HT after annealing. The q range between 0.19 and 0.3 \AA^{-1} is integrated for N2200 and the q range between 0.26 and 0.47 \AA^{-1} is integrated for P3HT. TA indicates after annealing at 260 °C for 30 min for FNDIT2/N2200 and at 100 °C for

10 min for FNDIT2/P3HT. Light blue and beige regions indicate the face-on and edge-on fractions, respectively.

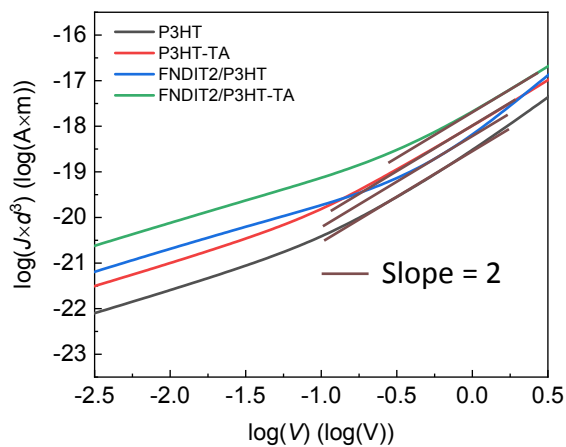


Fig. S9 Typical current density (J) normalized by thickness (d) plotted against voltage (V) in double logarithm scales. The lines are best fits to the SCLC model.

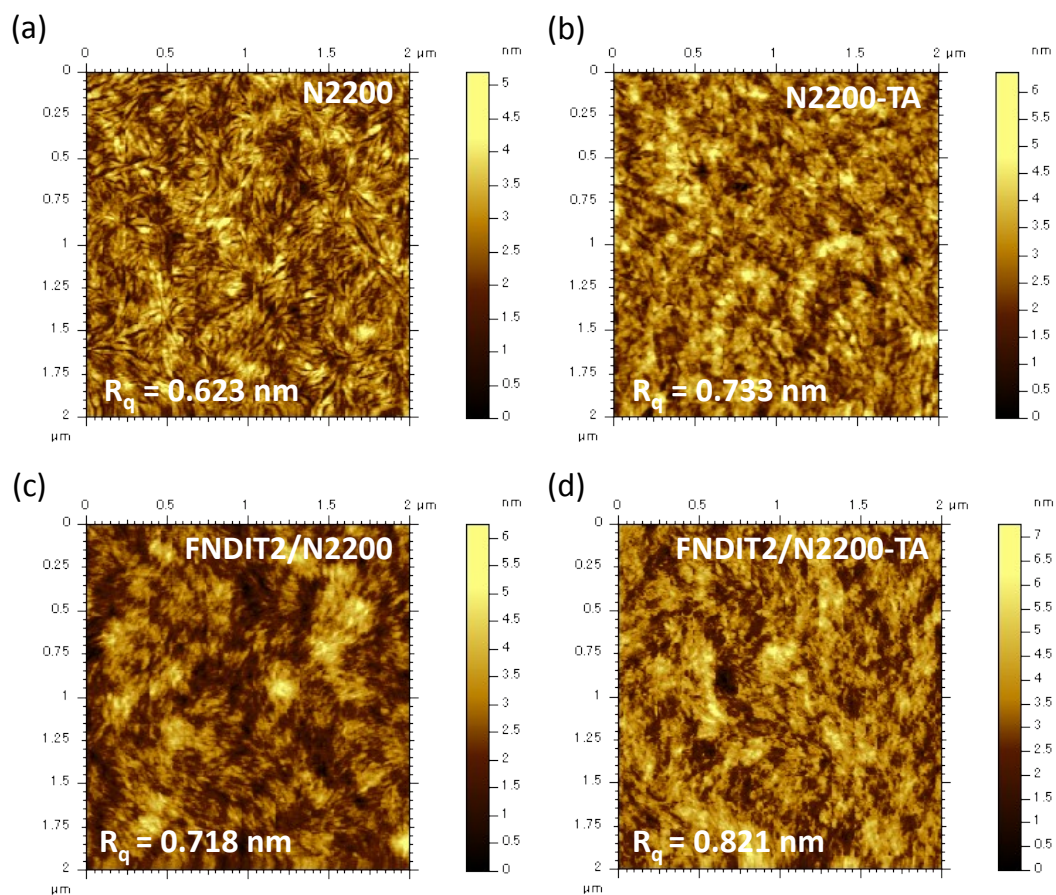


Fig. S10 AFM height images of (a) N2200, (b) N2200 after annealing at 260 °C for 30 min, (c) FNDIT2/N2200, and (d) FNDIT2/N2200 after annealing at 260 °C for 30 min.

The films were coated on Si/SiO₂ substrate. R_q : root-mean-square average of the height deviation.

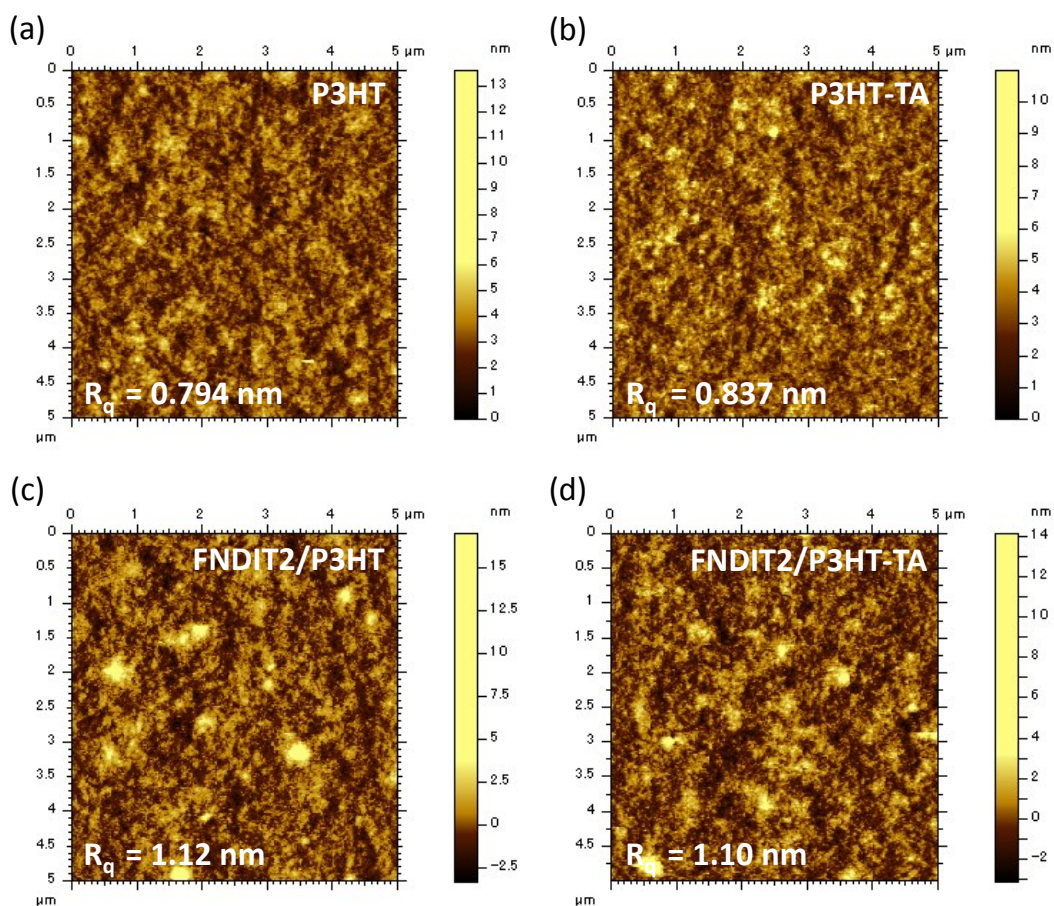


Fig. S11 AFM height images of (a) P3HT, (b) P3HT after annealing at 100 °C for 10 min, (c) FNDIT2/P3HT, and (d) FNDIT2/P3HT after annealing at 100 °C for 10 min. The films were coated on a Si/SiO₂ substrate. R_q : root-mean-square average of the height deviation.

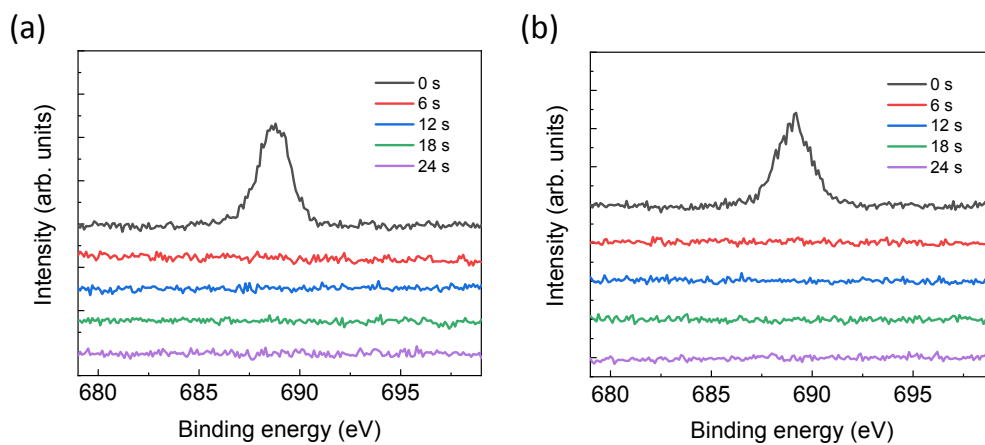


Fig. S12 XPS depth profiles of (a) FNDIT2/N2200 and (b) FNDIT2/P3HT films in the region of F 1s with different etching time from 0 s to 24 s.

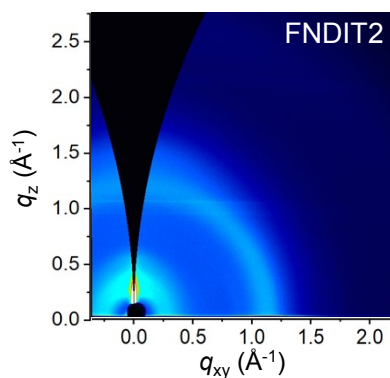


Fig. S13 2D GIWAXS patterns of the pure FNDIT2 film.

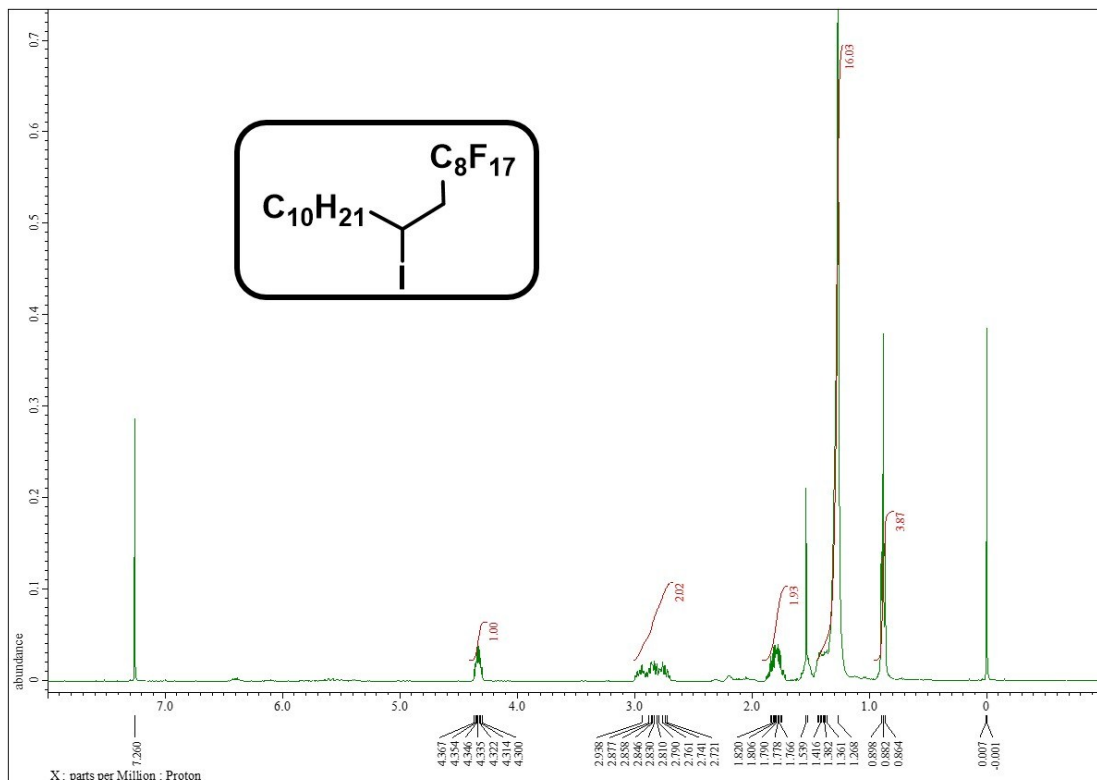


Fig. S14 ^1H NMR spectrum of 1.

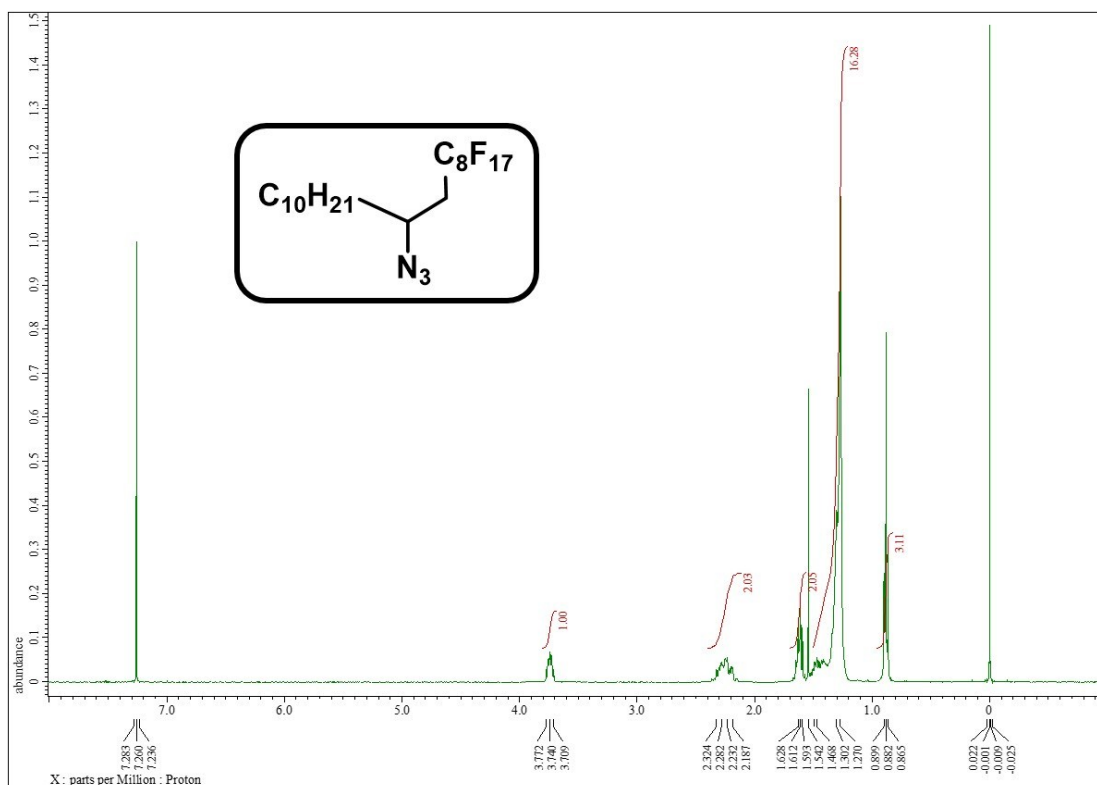


Fig. S15 ^1H NMR spectrum of 2.

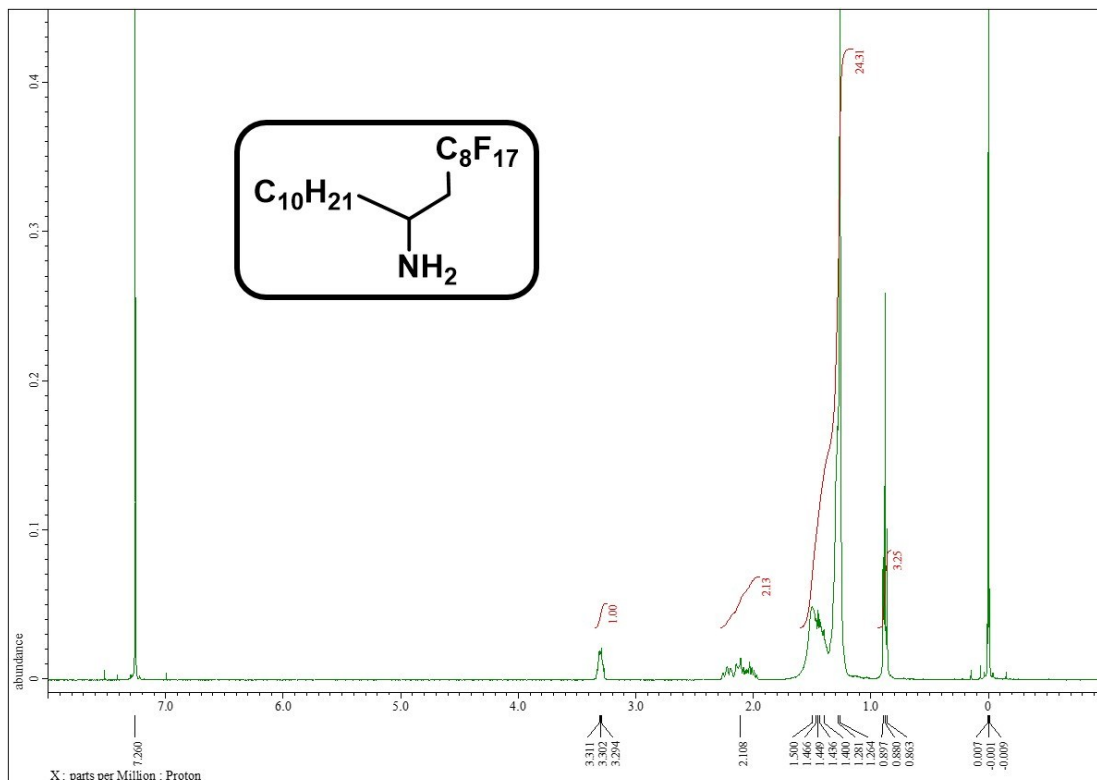


Fig. S16 ¹H NMR spectrum of 3.

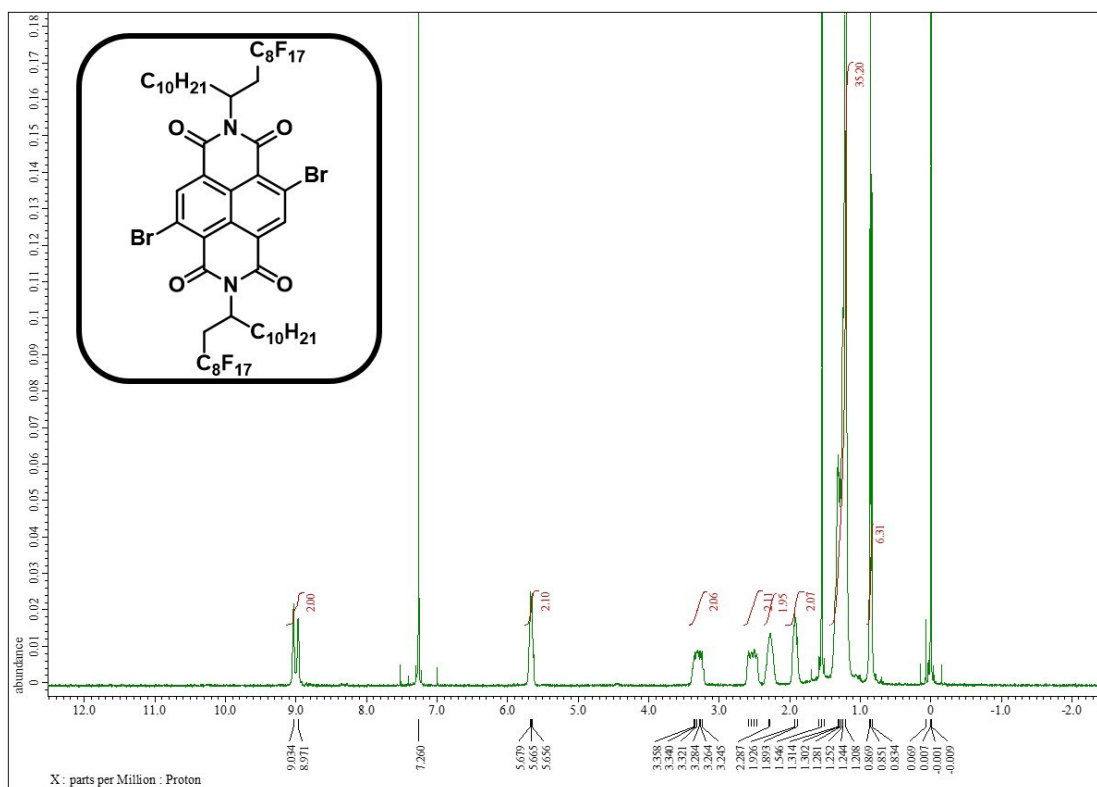


Fig. S17 ¹H NMR spectrum of 4.